MEGAFLOW – A NUMERICAL FLOW SIMULATION TOOL FOR TRANSPORT AIRCRAFT DESIGN

N. Kroll [1], C.C. Rossow [1], D. Schwamborn [1], K. Becker [2], G. Heller [3]

[1] DLR, Institute of Aerodynamics and Flow Technology, 38108 Braunschweig, Germany,
[2] Airbus-Deutschland GmbH, 28183-Bremen, Germany
[3] Fairchild-Dornier GmbH, 82234 Weßling, Germany

Keywords: *CFD capability based on block-structured and hybrid meshes, industrial applications*

Abstract

Some years ago the national CFD project MEGAFLOW was initiated in Germany, which combines many of the CFD development activities from DLR, universities and aircraft industry. Its goal is the development and validation of a dependable and efficient numerical tool for the aerodynamic simulation of complete aircraft. The MEGAFLOW software system includes the block-structured Navier-Stokes code FLOWer and the unstructured Navier-Stokes code TAU. Both codes have reached a high level of maturity and they are being intensively used by the German aerospace industry in the design process of a new aircraft. This paper highlights recent improvements and enhancements of the software. Its capability to predict viscous flows around complex industrial applications for transport aircraft design is demonstrated.

1 Introduction

Aerospace industry is increasingly relying on advanced numerical simulation tools in the early aircraft design phase. Nevertheless, there is still a great need for improvement of numerical methods, because standards for simulation accuracy and efficiency are constantly rising in industrial applications. Moreover, it is crucial to reduce the response time for complex simulations, although the relevant geometries and underlying physical flow models are becoming increasingly complicated.

In order to meet the requirements of German aircraft industry, the national project MEGAFLOW was initiated some years ago under the leadership of DLR [1],[2]. The main goal was to focus and direct development activities carried out in industry, DLR and universities towards industrial needs. The close collaboration between the partners led to the development and validation of a common aerodynamic simulation system providing both a structured and an unstructured prediction capability for complex applications. The software is constantly updated to meet the requirements of industrial implementations.

In the first phase of the project the main emphasis was put on the improvement and enhancement of the block-structured grid generator MegaCads and the Navier-Stokes solver FLOWer. In a second phase the activities were focused on the development of the unstructured/hybrid Navier-Stokes solver TAU. Due to a comprehensive and cooperative validation effort and quality controlled software development processes, both flow solvers have reached a high level of maturity and reliability. The MEGAFLOW software is used in the German aeronautic industry and research organizations for a wide range of applications. Due to the use of common software, the process of transferring latest research and technology results into production codes has been considerably accelerated.

The present paper describes the features of the software and demonstrates its capability on the basis of several applications from civil aircraft design.

2 MEGAFLOW Software

The MEGAFLOW software offers flow prediction capabilities which are based on both block-structured and hybrid meshes.

2.1 Grid Generation

For the generation of block-structured grids the interactive system MegaCads has been developed. Specific features of the tool are the parametric construction of multi-block grids with arbitrary grid topology, generation of high-quality grids through advanced elliptic and parabolic grid generation techniques, construction of overlapping grids and batch functionality for efficient integration in an automatic optimization loop for aerodynamic shape design. Details of the software are given in [3]. The limitation of MegaCads is the non automatic definition of the block topology which for rather complex configurations may result in a time consuming and labor intensive grid generation activity. Besides MegaCads, the commercial software package ICEM-HEXA and specialized in-house codes [4] are being used for specific applications.

In contrast to the block-structured approach, no major development activities have been devoted to the generation of unstructured meshes within the MEGAFLOW project. A strategic cooperation, however, has been established with the company CentaurSoft [5] which provides the hybrid grid generation package Centaur. The software consists of three major parts. An interactive program reads in the CAD data of the geometry under consideration, performs some CAD cleaning if necessary and sets up the grid generation process. In a second step the surface and volume grid are generated automatically. For viscous calculations a quasi-structured prismatic cell layer with a specified number of cells around the geometry surface ensures high resolution of boundary layer effects. In a third step grid adaptation may be used to locally refine grid resolution. During the cooperation the Centaur grid generation software has been substantially advanced for transport aircraft applications. Improvements include for example the generation of non isotropic elements and wake surfaces.

2.2 Flow Solvers

The main components of the MEGAFLOW software are the block-structured flow solver FLOWer and the unstructured hybrid flow solver TAU. Both codes solve the compressible, three-dimensional Reynolds-averaged Navier-Stokes equations for rigid bodies in arbitrary motion. The motion is taken into account by transformation of the governing equations. For the simulation of aeroelastic phenomena both codes have been extended to allow geometry and mesh deformation [6]. For multidisciplinary simulations the MPCCI-library [7] is used for the data exchange between the mono-disciplinary codes. In the following sections the specific features of the Navier-Stokes codes are briefly described.

Block-Structured Navier-Stokes Code FLOWer

The FLOWer-Code is based on a finite-volume formulation on block-structured meshes using either the cell vertex or the cell-centered approach. For the approximation of the convective fluxes a central discretization scheme combined with scalar or matrix artificial viscosity and several upwind discretization schemes are available [8]. Integration in time is performed using explicit multistage time-stepping schemes. For steady calculations convergence is accelerated by implicit residual smoothing, local time stepping and multigrid. Preconditioning is used for low speed flows. For time accurate calculations an implicit time integration according to the dual time stepping approach is employed. The code is highly optimized for vector computers. Parallel computations are based on MPI and they are realized through the use of a high level communication library [9].

A variety of turbulence models is implemented in FLOWer, ranging from simple algebraic eddy viscosity models over one- and two-equation models up to algebraic stress models. The Wilcox k-ω model is the standard model in FLOWer which is used for all types of applications. However, for transonic flow the linearized algebraic stress model LEA [10] recently has shown superior behavior with respect to other models [13]. All two-equation models can be combined with Kok's modification [11] for improved prediction of

vortical flows. For supersonic flows different compressibility corrections are available. Recently the nonlinear EARSM of Wallin [12] has been implemented and is currently under investigation.

Besides the modeling accuracy for turbulent flows, the numerical robustness of the respective transport equation turbulence models for complex applications has been a major issue. In FLOWer numerical stability is enhanced by an implicit treatment of the turbulence equations and different limiting mechanisms that can be activated by the user. The convergence behavior of the FLOWer-Code for a rather complex application is demonstrated in Fig. 1. Results of a viscous computation for a helicopter fuselage are shown [14]. The rotor is modeled through a uniform actuator disc. The grid consists of 94 blocks and 7 million grid points. The residuals for density and turbulence quantities are reduced several orders of magnitude. In this low Mach number case the preconditioning technique has been employed.

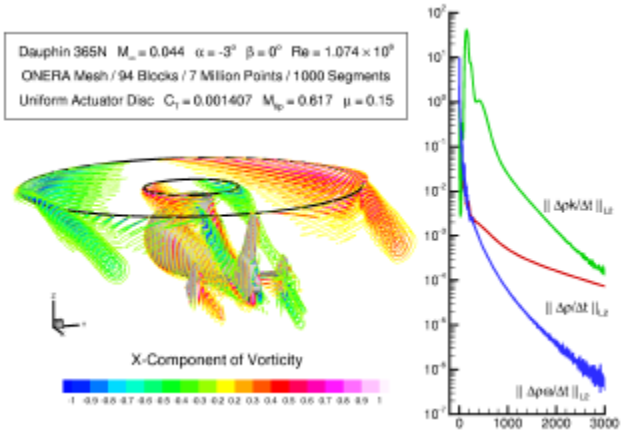

Fig. 1 Viscous calculation for Dauphin helicopter fuselage at M_∞=0.044, convergence behavior of mass and k-ω turbulence equations.

The fully implicit integration of the turbulence equations also ensures efficient calculations on highly stretched cells as they appear in high Reynolds number flows. Fig. 2 shows the convergence history of FLOWer for the calculation of the viscous flow around the RAE 2822 airfoil at different Reynolds numbers. The advantage of the fully implicit method compared to the explicit multigrid scheme with point implicit treatment of source terms is evident.

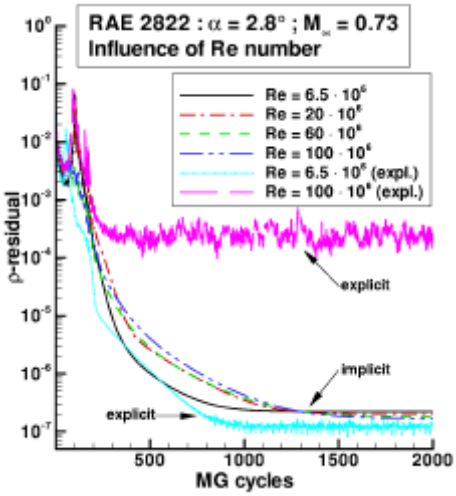

Fig. 2 Effect of Reynolds number on convergence for the RAE 2822 airfoil at M_∞=0.73, α=2.8^0.

FLOWer is able to perform transition prediction on airfoils using a module consisting of a laminar boundary layer code and an e^N-database method based on linear stability theory [15]. Fig. 3 shows the predicted and measured force polars and transition locations of a subsonic laminar airfoil. This approach substantially improves the quality of predicted force coefficients. The experimentally determined transition points are reproduced with high accuracy. The transition prediction capability is currently extended to wings and 2D high-lift systems.

An important feature of FLOWer is the Chimera technique, which considerably enhances the flexibility of the block-structured approach [16],[17]. This technique enables the generation of a grid around a complex configuration by decomposing the geometry into less complex components. Separate component grids are generated which overlap each other and which are embedded in a Cartesian background grid that covers the whole computational domain. In combination with flexible meshes, the Chimera technique enables an efficient way to simulate bodies in relative motion. The communication from mesh to mesh is realized through interpolation in the overlapping area. The search for cells which are used for interpolation is performed using an alternating digital tree method. In the case when

a mesh overlaps a body which lies inside another mesh, hole cutting procedures have to be used in order to exclude the invalid points from computation.

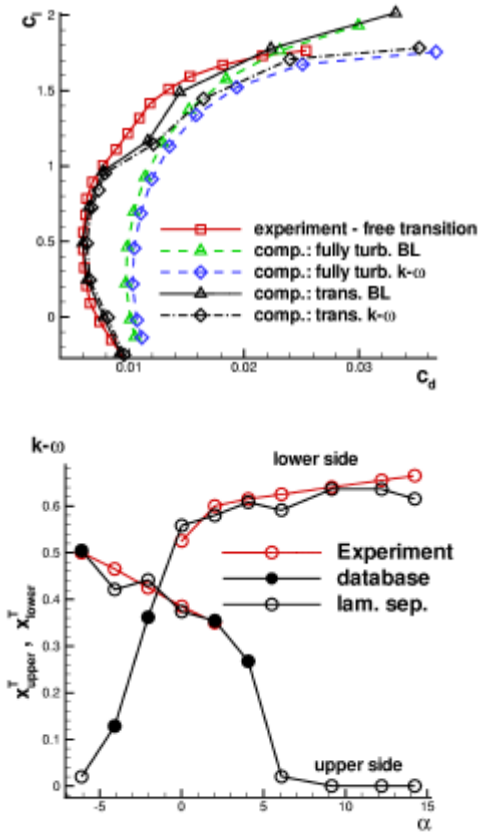

Fig. 3 Transition prediction with e^N-database method for laminar Sommers airfoil at M_∞=0.1 and Re=4x10^6, (a) force polars calculated fully turbulent and with transition, (b) computed and measured transition locations.

Further simplification of the grid generation procedure is achieved by a fully automatic Cartesian grid generator. The grid generator places fine grids around the component grids and puts successively coarsened grids around the fine grids. Patched grid interfaces with hanging nodes are used at the interface between the grid blocks of the Cartesian mesh. In the vicinity of the configuration the Cartesian grid generator creates non isotropic cells which are adapted to the size of the cells in the component grids. This ensures accuracy in the overlap regions. The potential of the Chimera technique is demonstrated in Fig. 4 in case of the viscous calculation around a 3D high-lift configuration. Separate component grids have been generated for body, wing, flap and slat. The background grid has been produced with the automatic Cartesian grid generator. With this approach the time for grid generation has been considerably reduced. The whole grid consists of 4 million points in total. The enlarged view around the slat and the leading edge of the main wing shows that flow quantities are not disturbed by the grid interfaces.

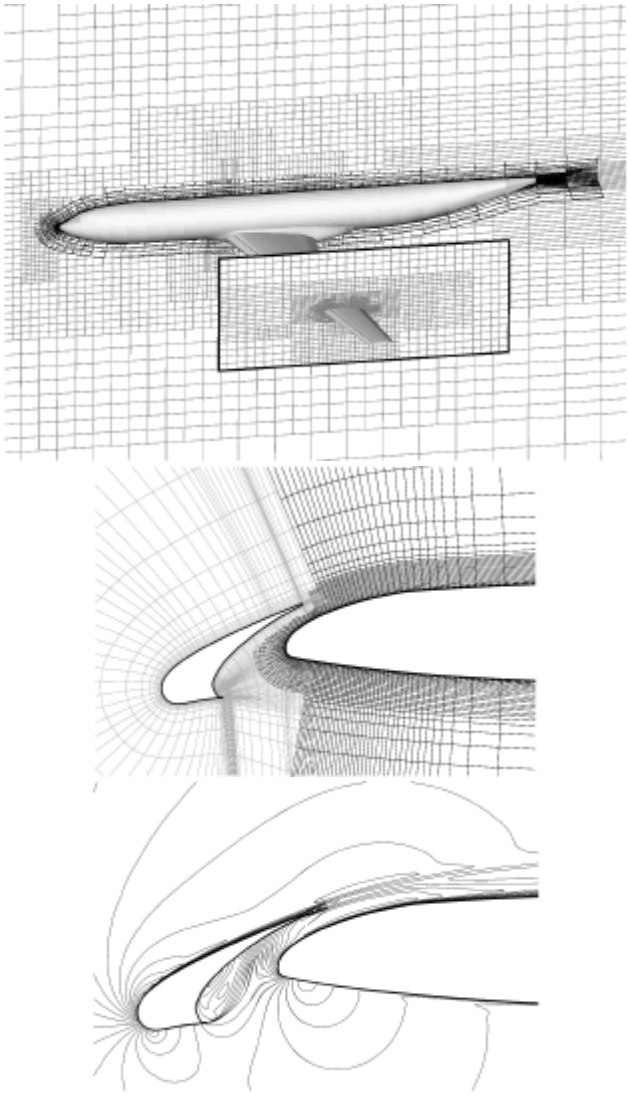

Fig. 4 Viscous computation around a 3D high-lift configuration using the Chimera technique of the block-structured FLOWer-Code, M_∞=0.174, $\alpha=7^0$

For shape optimization, FLOWer offers an inverse design mode which is based on the inverse formulation of the small perturbation method according to Takanashi [18]. The method has been extended to transonic flows

[19] and is capable of designing airfoils, wings and nacelles in inviscid and viscous flows. This strategy is very efficient, however, it is restricted to a prescription of a target pressure distribution. In order to support shape optimization based on more general cost functions and constraints, the continuous adjoint approach based on the work of Jameson [20] has been implemented in FLOWer [21]. With the solution of the adjoint flow equations the gradients of the cost functions can be efficiently calculated independent of the number of design variables. Since the adjoint and flow equations are solved in a similar way, all features of the main FLOWer-Code are available in the adjoint solver. Therefore, complex 3D multi-block geometries with arbitrary parametrization can be handled, as well as aerodynamic constraints and multi-point designs. The adjoint approach is currently extended to the Navier-Stokes equations.

Hybrid Navier-Stokes Code TAU

The Navier-Stokes code TAU [22] makes use of the advantages of unstructured grids. The mesh may consist of a combination of prismatic, pyramidal, tetrahedral and hexahedral cells and therefore combine the advantages of regular grids for the accurate resolution of viscous shear layers in the vicinity of walls with the flexibility of grid generation techniques for unstructured meshes. The use of a dual mesh makes the solver independent of the type of cells that the initial grid is composed of. Various spatial discretization schemes were implemented, including a central scheme with artificial dissipation and several upwind methods. In order to accelerate convergence, a multigrid procedure was developed based on the agglomeration of the control volumes of the dual grid for coarse grid computations.

In order to efficiently resolve detailed flow features, a grid adaptation algorithm for hybrid meshes based on local grid refinement and wall-normal mesh movement in semi-structured near-wall layers was implemented. This algorithm has recently been extended to allow also for de-refinement of earlier refined elements thus enabling the code to be used for unsteady time-accurate adaptation in unsteady flows. Fig. 5 gives a simple example of the process for viscous airfoil calculation. First a flow solution is calculated on a basic grid (a). After some refinement an adapted grid/solution is obtained (b). Changing the flow parameters and specifying e.g. that the number of mesh points should not increase any further, the de-refinement interacts with the refinement (c) and finally the new shock position is resolved (d).

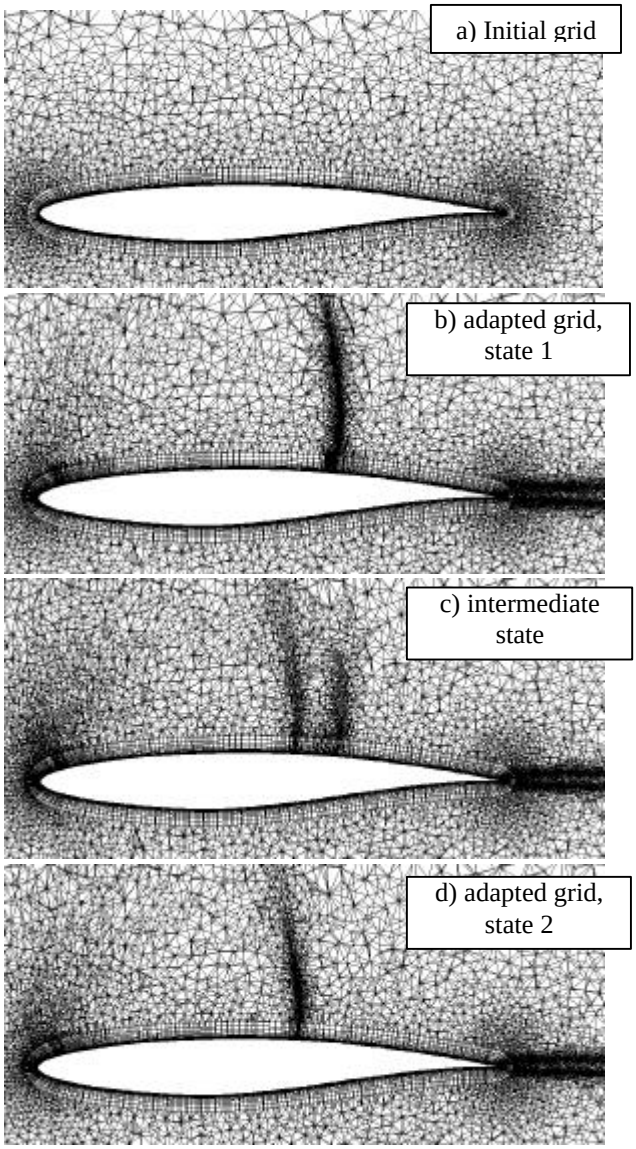

Fig. 5 Dynamic mesh adaptation.

With respect to unsteady calculations, the TAU-Code was extended to simulate a rigid body in arbitrary motion and to allow grid deformation. In order to bypass the severe time-step restriction associated with explicit schemes,

the implicit method based on the dual time stepping approach was implemented. For the calculation of low-speed flows, preconditioning of the compressible flow equations similar to the method used in FLOWer was implemented. One of the important features of the TAU-Code is its high efficiency on parallel computers. Parallelization is based on the message passing concept using the MPI-library [9]. The code is further optimized either for cache or vector processors through specific edge coloring procedures.

The standard turbulence model in TAU is the Spalart-Allmaras model with Edwards modification, yielding highly satisfactory results for a wide range of applications while being numerically robust. Besides this model, a number of different k-ω models with and without compressibility corrections are available. Also the linearized algebraic stress model LEA [10] has recently been integrated.

As the Chimera technique has been recognized as an important feature to efficiently simulate maneuvering aircraft, it has been also integrated into the TAU-Code [23]. In the context of hybrid meshes the overlapping grid technique allows an efficient handling of complex configurations with movable control surfaces (see Fig. 6).

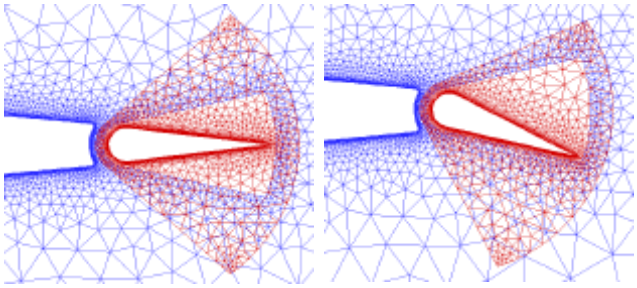

Fig. 6 Hybrid Chimera grid for delta wing with a movable control surface.

For the intergrid communication linear interpolation based on a finite element approach is used in case of tetrahedral mesh elements. For other types of elements (prisms, hexahedrons, pyramids) linear interpolation is performed by splitting the elements into tetrahedrons. Like in FLOWer, the search algorithm for donor cells is based on the alternating digital tree data structure. The current implementation of the Chimera technique can handle both steady and unsteady simulations for inviscid and viscous flows with multiple moving bodies. The technique is currently restricted to the sequential mode of the TAU-Code. In Fig. 7 results of a viscous Chimera calculation for a delta wing with trailing edge flaps are shown. The component mesh of the flap is designed to allow a flap deflection of $\pm 15^0$. The comparison of calculated and measured surface pressure distributions at both 60% and 80% cord length shows a good agreement.

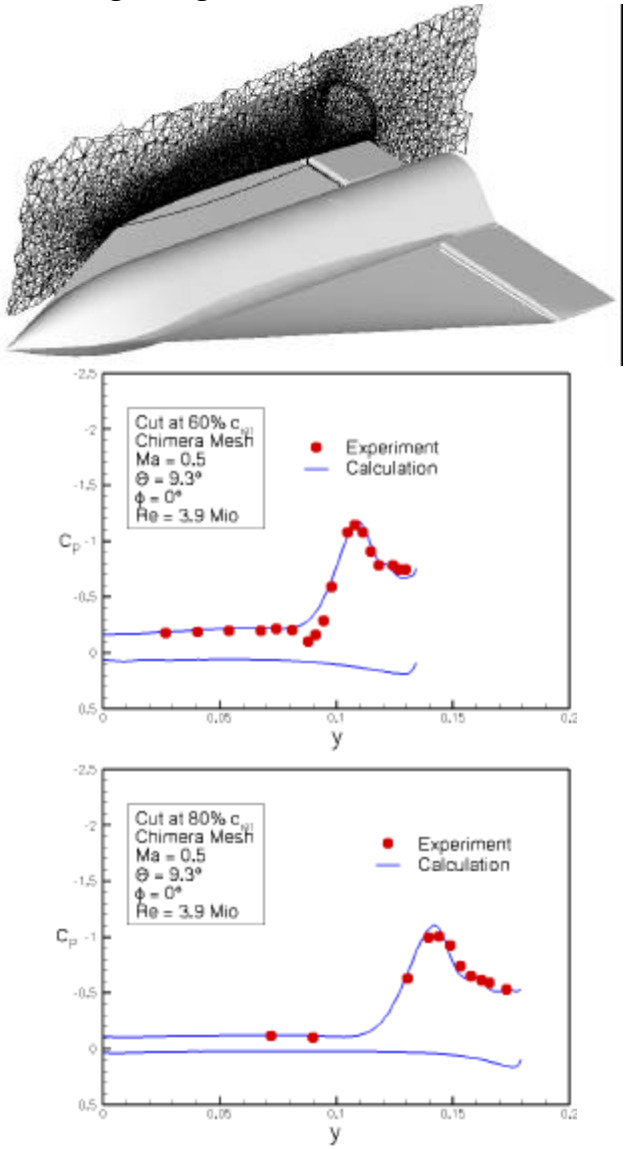

Fig. 7 Viscous computation of a delta wing with trailing edge flap using the Chimera option of the hybrid TAU-Code, surface pressure distributions for flap deflection angle $\theta=0^0$ at 60% and 80% cord.

3 Software Validation

Software validation is a central and critical issue for providing reliable CFD tools for industrial applications. Among others, the validation exercises should address consistency of the numerical methods, accuracy assessment for different critical application cases and sensitivity studies with respect to numerical and physical parameters. Best practice documentation is an essential part of the work. Over the last few years the MEGAFLOW software was validated for a wide range of configurations and flow conditions (see e.g. [2],[25],[26]). This section deals with recent results for a subsonic and transonic validation test case.

Flow prediction for a transport aircraft in high-lift configuration is still a challenging problem for CFD. The numerical simulation addresses both complex geometries and complex physical phenomena. The flow around a wing with deployed high-lift devices at high incidence is characterized by the existence of areas with separated flow and strong wake/boundary layer interaction. The capabilities of the MEGAFLOW software to simulate two- and three-dimensional high-lift transport aircraft configurations has been extensively validated within the European high-lift programme EUROLIFT [27]. One of the investigated test cases is the DLR-F11 wing/body/flap/slat-configuration (Fig. 8).

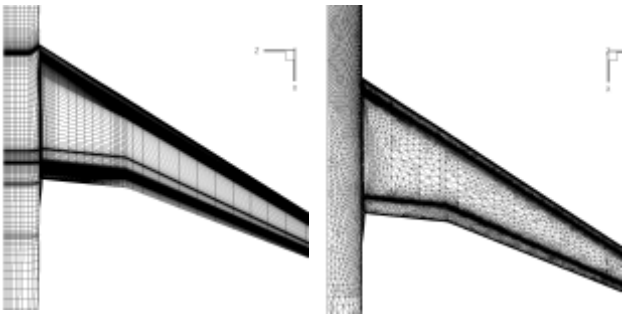

Fig. 8 Structured and unstructured surface grid for DLR-F11 high-lift configuration.

The left part of Fig. 8 shows a block-structured surface grid for the take-off configuration whereas on the right hand side an unstructured grid for the landing configuration is presented. Fig. 9 highlights a comparison of lift and total drag results of the unstructured TAU-Code and the block-structured FLOWer-Code with experimental data from the Airbus LWST low speed wind tunnel in Bremen, Germany. Both, the block-structured grid generated by the DLR software MegaCads and the hybrid mesh generated by FOI contain about 3 million grid points to allow for a fair comparison of the methods.

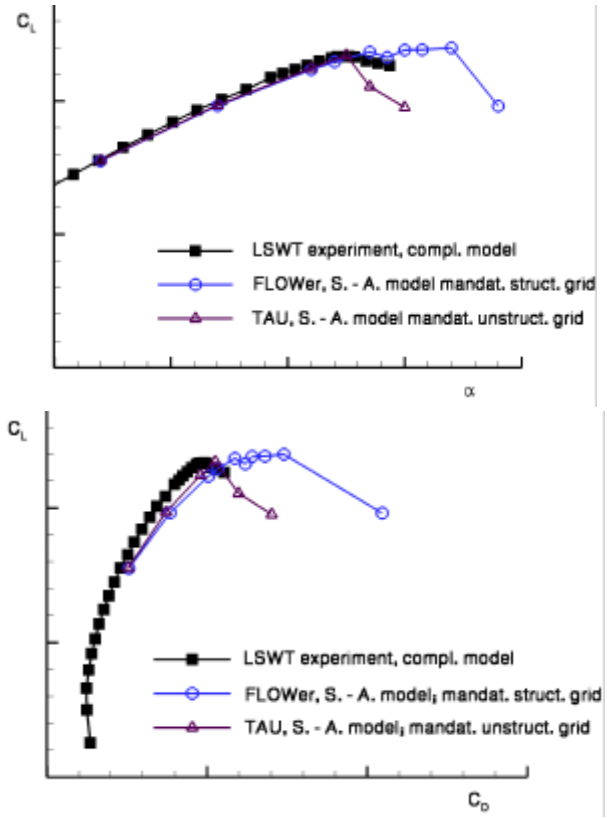

Fig. 9 Viscous computations for DLR-F11 high-lift configuration at M_∞=0.18, Re=1.4x106, lift as function of angle of attack and as function of drag.

Calculations for the start configuration at M_∞=0.18 and Re=1.4x10^6 were performed with FLOWer and TAU using the Spalart-Allmaras turbulence model with Edwards modification (SAE). In both cases preconditioning was used to speed-up steady state convergence and to improve accuracy at the predominantly low speed conditions. In the linear range of the polar, the numerical results compare quite well with each other and with experimental data. At higher angle of attack differences occur between the TAU and FLOWer results. TAU predicts the lift break down at a lower angle of attack. The

lack of mesh resolution in the hybrid grid is considered to be the main reason for this difference.

In the framework of the AIAA CFD Drag Prediction Workshop [24], the accuracy of the MEGAFLOW software was assessed to predict aerodynamic forces and moments for the DLR-F4 wing-body configuration [13]. In Fig. 10 lift coefficient as function of drag and angle of attack for Case 2 (M_∞=0.75, Re=3x10^6) calculated with FLOWer and TAU are presented. These results were obtained using grids generated in-house at DLR. On request all calculations were performed fully turbulent. The FLOWer computations were carried out on a grid with 3.5 million points using central discretization with a mixed scalar and matrix dissipation operator and the k/ω-LEA turbulence model. The TAU results are based on an initial grid containing 1.7 million points which was adapted for each angle of attack yielding grids with 2.4 million points. In addition, an adaptation of the prismatic grid towards Y^+=1 was done. Central discretization with standard settings of artificial dissipation was used. Turbulence was modeled with the one-equation model of Spalart-Allmaras. As can be seen from Fig. 10 the fully turbulent FLOWer computations overpredict the measured drag curve by approximately 20 drag counts. Investigations have shown [13] that inclusion of transition in the calculation reduces the predicted drag by 14 drag counts, reducing the overprediction of drag to approximately 6 drag counts. The results of the unstructured fully-turbulent computations with TAU perfectly match with the experimental data. However, as for the structured computations, hybrid calculations with transition setting will reduce the predicted level of drag, in this case by approximately 10 drag-counts. Fig. 10 also shows the comparison of predicted and measured lift coefficient as a function of angle of attack. The values calculated by FLOWer agree very well with the experiment, whereas the results obtained with TAU overpredict the lift almost in the whole range of angle of attack.

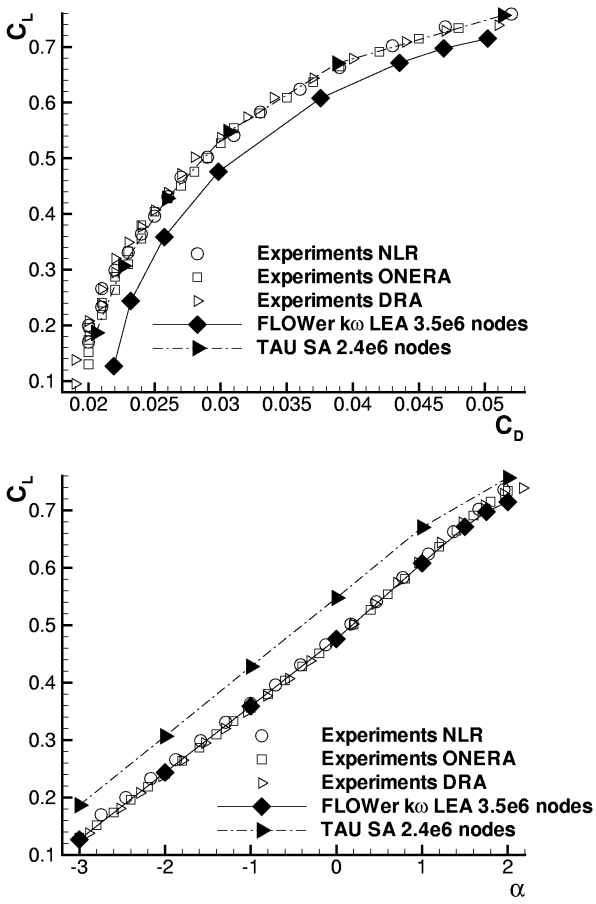

Fig. 10 Viscous calculations for DLR-F4 wing/body configuration (AIAA drag prediction workshop, case 2), $C_L(C_D)$, $C_L(\alpha)$.

For the pitching moment (Fig. 11) the results obtained with FLOWer agree very well with experimental data. This is due to the fact that the surface pressure distribution predicted with the FLOWer-Code is in good agreement with the experiment. In case of the hybrid TAU-Code there are some discrepancies between the predicted and measured surface pressures resulting in a significant overprediction of the pitching moment. Further investigations [13] have shown that the improved results obtained with the FLOWer-Code are mainly attributed to a lower level of numerical dissipation (improved grid resolution and matrix dissipation) combined with the advanced 2-equation k/ω-LEA turbulence model.

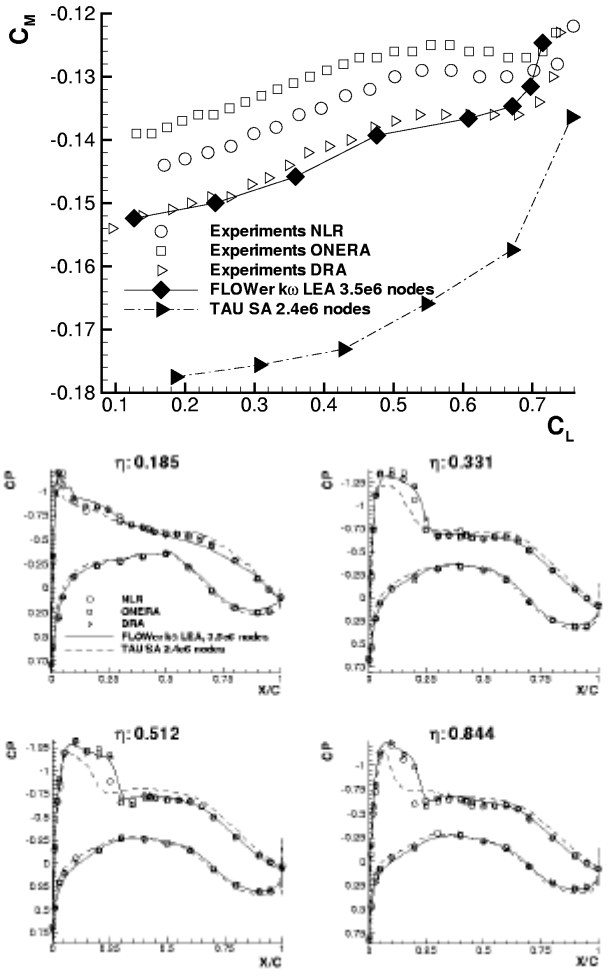

Fig. 11 Viscous calculations for DLR-F4 wing/body configuration (AIAA Drag Prediction Workshop, case 2), $C_M(C_L)$ polar and surface pressure distribution for C_L=0.5.

4 Industrial Applications

The MEGAFLOW software is intensively used at DLR and the German aircraft industry for many aerodynamic problems. Some typical large scale applications listed below shall demonstrate the capability of the software to support civil aircraft design.

4.1 Low Speed Flows

At Airbus Deutschland, calculations have been carried out for a wing/body/slat/flap high-lift configuration. This configuration is designed to produce data for the complete range of incidences, especially around maximum lift, for low and high Reynolds numbers.

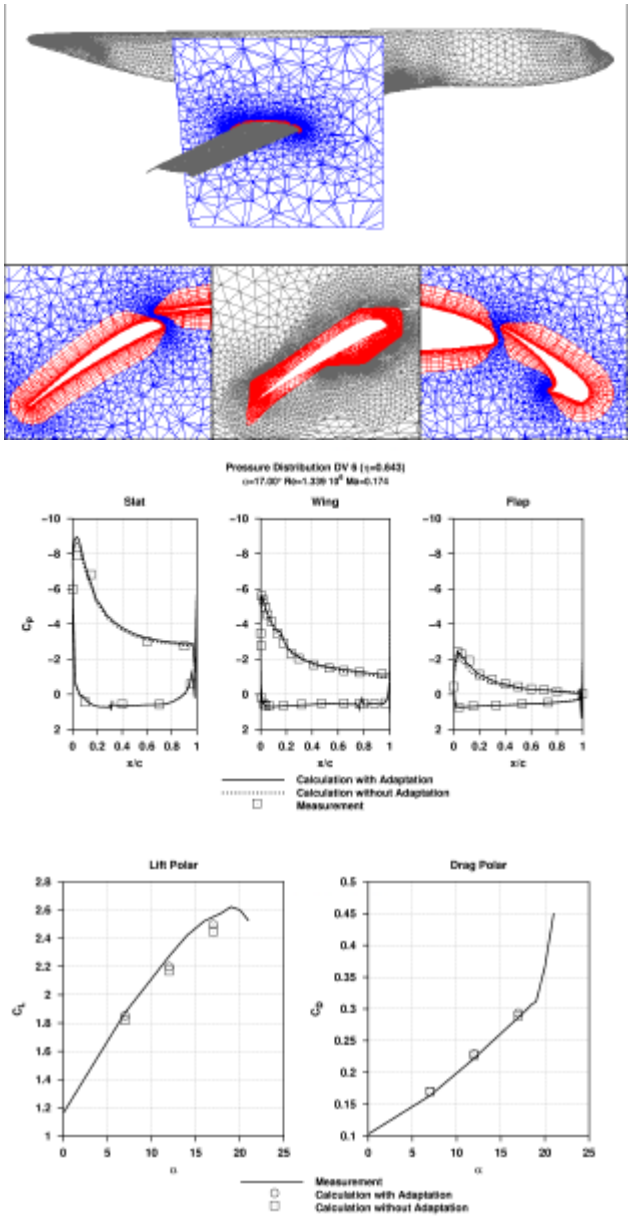

Fig. 12 Results of the hybrid TAU-Code for a 3d high-lift landing configuration at M_∞=0.18, Re=1.4x10^6, (a) hybrid grid with 8 million points, (b) lift and drag as function of angle of attack, (c) surface pressure distribution for $\alpha=17^0$.

For simplicity, slat and flap of the wing are covering the whole wing span, without any gap at the body or kink (Fig. 12a). Viscous computations were done for the landing configuration with the hybrid TAU-Code using the Spalart/Allmares turbulence model with Edwards modification. The mesh with prismatic layers near the aircraft surface is produced by Centaur. During the calculation it is adapted towards Y^+=1 for the first mesh cell. The grid

consists of 8 million points. Pressure distributions for all three wing elements at angle of attack $\alpha=17^0$ and the aerodynamic forces show an excellent agreement with experimental data Fig. 12. For these calculations 64 CPUs of the Hitachi SR8000 computer were used. The computation time for one polar point was 17 h.

At DLR, effort is concentrated to explore the applicability of the hybrid TAU-Code to configurations beyond wing/body [28].

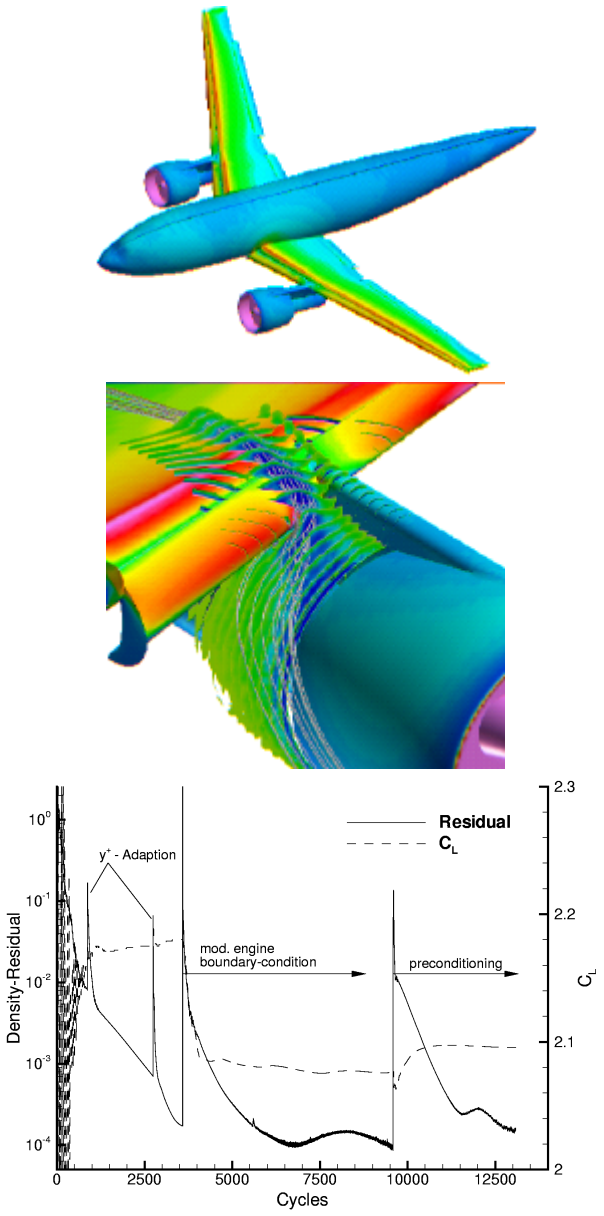

Fig. 13 Viscous simulation of the ALVAST high-lift configuration with UHBR engine using TAU, (a) surface pressure distribution, (b) nacelle vortex, (c) convergence history.

For the DLR ALVAST model equipped with an advanced UHBR (Ultra High Bypass Ratio) engine, numerical simulations are focused on complex flow phenomena arising from the engine installation at high-lift conditions. Special attention is paid to possible reductions of the maximum lift angle by means of dominating three-dimensional effects due to engine installation. Fig. 13a displays the surface pressure coefficient of the ALVAST high-lift configuration with installed UHBR engine at an angle of attack of $\alpha=12°$ in take-off conditions. The computation was performed on a hybrid grid with 10 million points generated by Centaur. In Fig. 13b the vortex shedding from the inboard side of the nacelle is shown. The vortex originates from the rolling-up of the shear layer and it crosses the slat and the wing upper side. Using the computational data as input in a recent wind tunnel campaign, this vortex system could be identified with PIV visualization. The research carried out in this context led to an improvement in engine boundary conditions on hybrid meshes and to an improved applicability of low speed preconditioning to complex configurations. Fig. 13c shows the convergence history of the computation. Despite the high complexity of the flow, a satisfying convergence of the density residual of about four orders of magnitude is achieved.

The applicability of the hybrid TAU-Code to complex industrial configurations is demonstrated for wing/body configurations with engine nacelles and deployed high-lift system (Fig. 14). Due to the double slotted flaps and corresponding flap tracks, the geometry is quite complex. One of the objectives of these computations was to identify the influence of the nacelles on the flow over the wing. In Fig. 14b streamlines on the surface indicate strong influence already at an angle of attack of $\alpha=4°$. The applicability of numerical simulation to such geometrically and physically complex configurations can be assessed from Fig. 14c where a comparison of lift as a function of angle of a attack is shown for experimental and

computational results at M_∞=0.174 and Re=1.246x10^6.

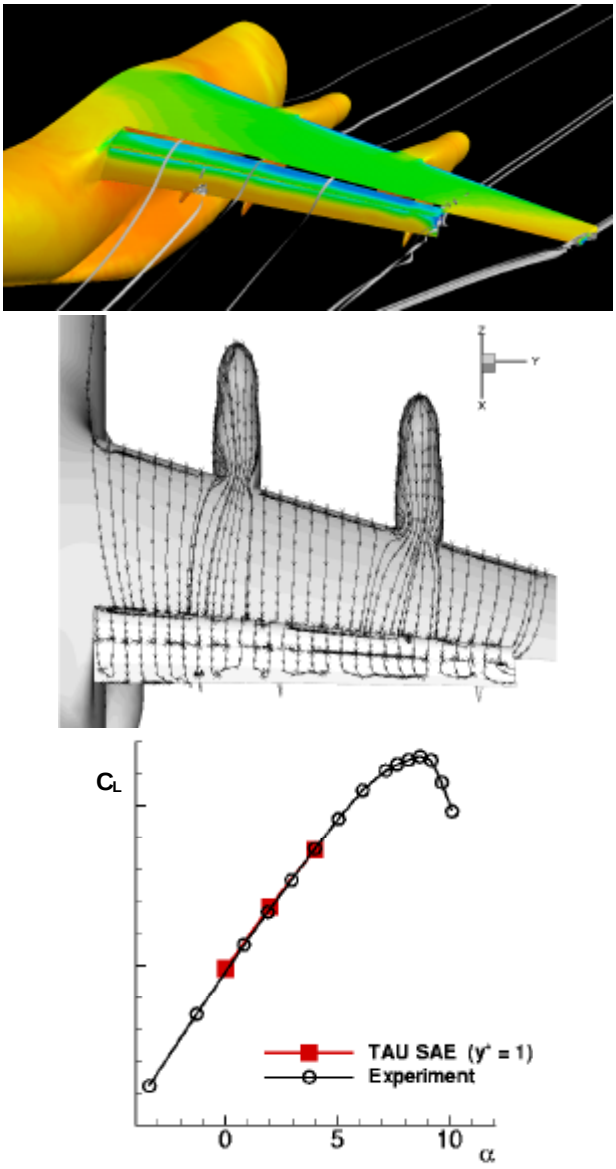

Fig. 14 Results of viscous calculations with the hybrid TAU-Code for high-lift configuration, M_∞=0.174, Re=1.246x10^6, (a) surface pressure, (b) streamlines on the upper side of the wing, (c) lift coefficient as function of angle of attack.

In order to assess the capability of Gurney flaps to change flow characteristics of wings, the TAU-Code was employed to compute the flow around an airfoil with different Gurney flap geometries. The flap under investigation could be deployed at angles varying between 0° and 90°. Fig. 15a displays the hybrid computational grid around the Gurney flap with 30° deployment angle. The simulation allows a detailed analysis of the flow phenomena close to the trailing edge device (Fig. 15b). The ability of the numerical simulation to correctly predict the influence of Gurney flaps on the global airfoil flow is demonstrated in Fig. 15c.

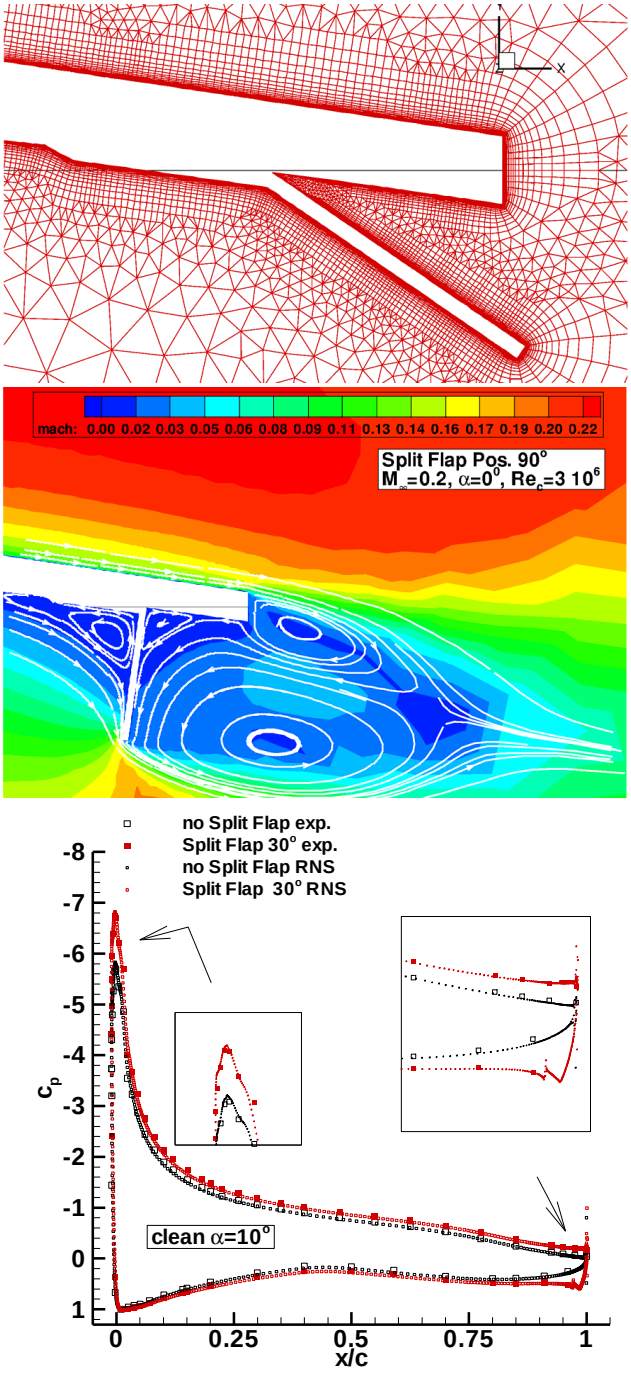

Fig. 15 Numerical simulation of airfoil with Gurney flap using the TAU-Code, (a) hybrid grid for deployment angle of δ=30^0, (b) Mach number distribution and streamlines for δ=90^0, (c) predicted and measured surface pressure distributions for δ=0^0 and δ=30^0.

Experimental and computational pressure distributions are shown for Gurney flap deployment angles of 0° and 30°. Note, that details at the leading and trailing edge are consistently predicted.

For a large transport aircraft configuration the effect of winglets on take-off performance was to be assessed. Fig. 16 gives a view of the configuration with and without winglets.

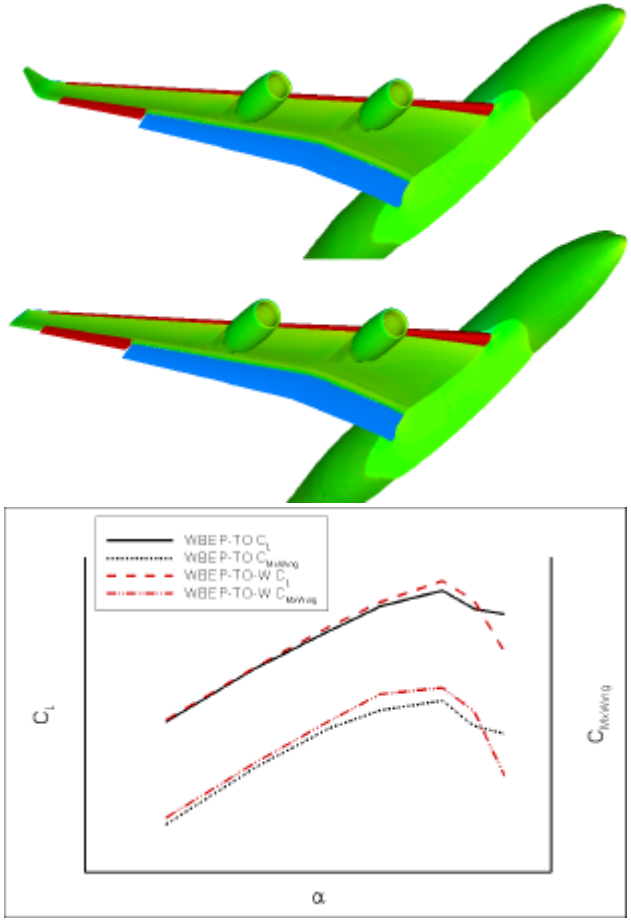

Fig. 16 Prediction of winglet effect on take-off performance of large transport aircraft based on viscous flow simulations using the TAU-Code, (a) configuration with and without winglet, (b) lift and root bending moment as function of angle of attack, M_∞=0.2, Re=5.25x10^6.

For this study viscous flow simulations using the TAU-Code were conducted at M_∞=0.2 and Re=5.25x10^6. The calculations were performed on a hybrid grid with 8.5 million nodes using the Spalart/Allmares turbulence model with Edwards modification. In Fig. 16 the improvement of C_{Lmax} for the configuration with winglet can be identified. However, this gain in aerodynamic performance has to be balanced against structural consequences. In Fig. 16 also the computed root bending moment for the two configurations is given as function of angle of attack. In a more detailed analysis of the aircraft as an integrated system, the aerodynamic benefit has to be checked against the increased root bending moment due to winglet installation.

4.2 High Speed Flows

Airbus Deutschland is using Euler/RANS calculations to compute aerodynamic loads on all aircraft components. While formerly these data had to be derived from wind tunnel experiments with rather expensive models, CFD now offers the possibility to locally analyze the behavior of aerodynamic forces at any flow condition in an early stage of the development process. Fig. 17 shows the normal force along the axis of the aircraft body, calculated with the block-structured FLOWer-Code at M_∞=0.85 and angle of attack α=0^0.

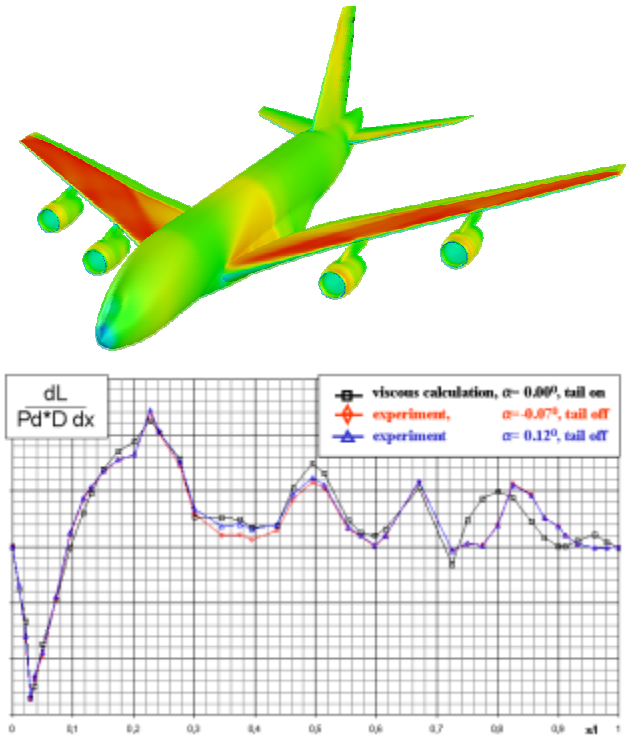

Fig. 17 Prediction of local normal force distribution along fuselage of civil transport aircraft at M_∞=0.85 and angle of attack α=0^0, comparison of FLOWer results with experimental data.

The computation was performed on a grid with 32 blocks and 8 million nodes. For comparison experimental results at nearby angles of attack are plotted. Major differences can only be seen in the rear fuselage area. The experiment was conducted with tails off while the computation was carried out with tails on.

One key issue during the design of an enhanced civil aircraft is the efficient engine-airframe integration. Modern very high-bypass ratio engines and the corresponding close coupling of engine and airframe may lead to substantial loss in lift and increased installation drag.

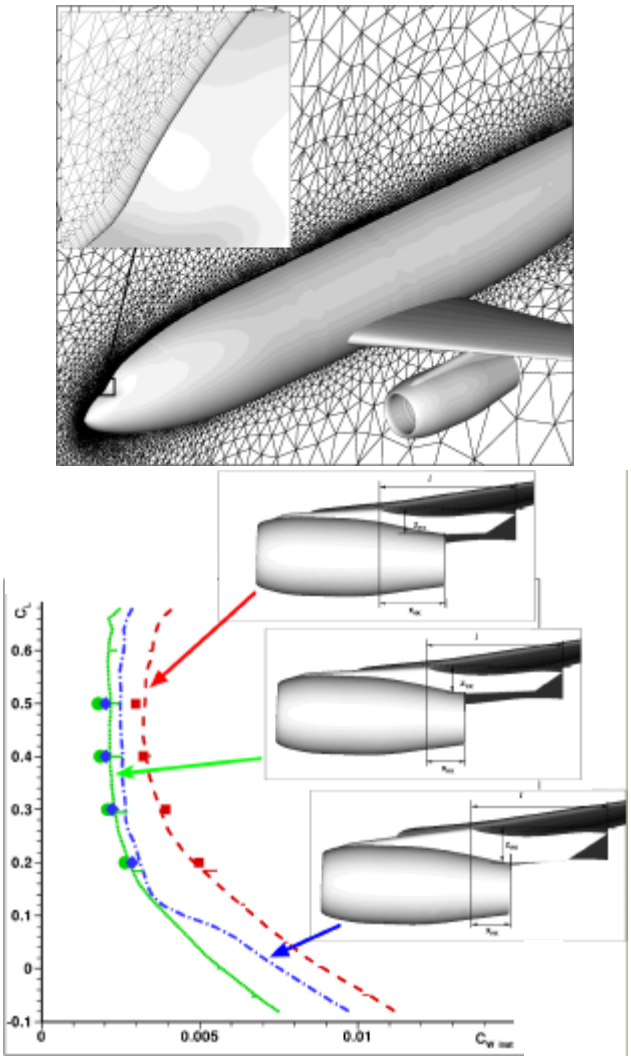

Fig. 18 Prediction of engine-airframe interference drag using the TAU-Code, (a) hybrid grid for DLR-F6 configuration, (b) lift as a function of installation drag for three different position of CFM56 engine, M_∞=0.75, Re=3x10^6, symbols: calculation, lines: experiment.

At DLR, numerical and experimental studies have been devoted to estimate installation drag with respect to variations of engine concepts and the installation positions [29], [30]. For numerical investigations in this field both the block-structured FLOWer-Code and the hybrid TAU-Code have been used. Fig. 18a shows the hybrid grid in the symmetry plane for the DLR-F6 configuration. The initial grid generated with Centaur consists of about 4.6 million nodes. Several solution based grid adaptation steps have been performed resulting in grids between 7.5 and 8.5 million nodes depending on the investigated engine concept. In Fig. 18b the lift as a function of the installation drag is plotted for three different positions of the CFM56 long duct nacelle (M_∞=0.75 and Re=3x10^6). The engines are represented by through-flow nacelles. Results predicted with the TAU-Code (symbols) and measured in the ONERA S2MA wind tunnel (lines) are shown. The agreement is very satisfactory demonstrating that the influence on installation drag due to varying engines locations or sizes can be accurately predicted by TAU [29].

Viscous computations with the block-structured FLOWer-Code were performed for the DLR-ALVAST configuration with turbofan engines for the usually most interesting conditions ‘Start of Cruise’ (SOC) and ‘Through Flow Nacelle’ (TFN) representing a flight-idle power setting [30]. Computations were carried out at M_∞=0.75, Re=3x10^6 and with a constant lift coefficient of C_L=0.5. Fig. 19 shows the impact of the power setting. Computed lines of constant Mach number in the engine symmetry plane are shown. The primary differences caused by the SOC thrust condition are the strong velocity increase in the jets up to supersonic speed and the resulting significant shear layers at the jet boundaries due to the larger velocity differences. Fig. 19 also shows corresponding computed and measured pressure distributions at the wing cross section η=33% (inboard of nacelle). The most significant difference between the SOC and TFN condition is a lower pressure level for SOC in the mid chord area at the wing lower side. This

influence is captured quite well by the numerical simulation.

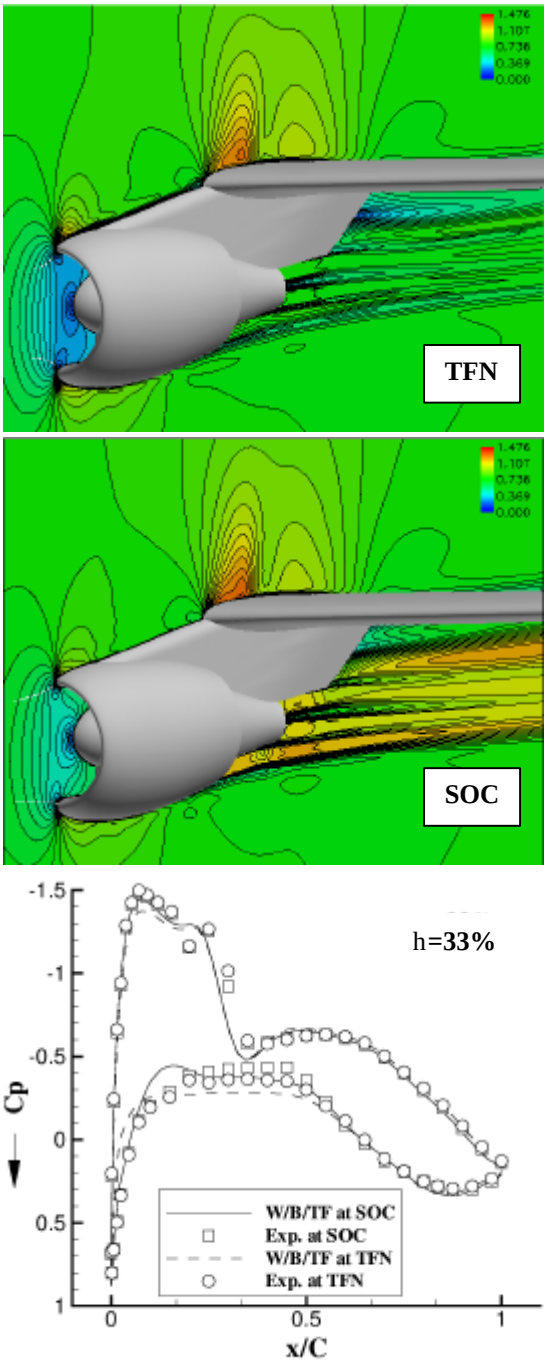

Fig. 19 Viscous calculation of DLR ALVAST configuration with FLOWer at M_∞=0.75, C_L=0.5, influence of thrust condition of turbofan engine, (a) and (b) constant Mach number distribution for TFN and SOC , (c) surface pressure distribution at cross section η=33%.

The influence of the jet vanishes for outer cross sections. Drag decomposition, a unique feature of Navier-Stokes computations, for the different engine conditions have shown [30] that the strongest influence of the thrust condition is found on the nacelle for pressure drag and less severe for friction drag.

Another application of the MEGAFLOW software at industry is the investigation of the effectiveness of control surfaces such as spoilers and ailerons for cruise conditions. Navier-Stokes calculations with the Chimera option of the block-structured FLOWer-Code were performed for a wing/body configuration including a spoiler at different deflection angles [31]. The grid system consists of two separate meshes, the background mesh around the clean wing/body configuration (single block with CO topology and 2.8 million nodes) and the component mesh around the spoiler (3 blocks with CH-topology and 0.5 million mesh) which was embedded inside the background mesh (see Fig. 20).

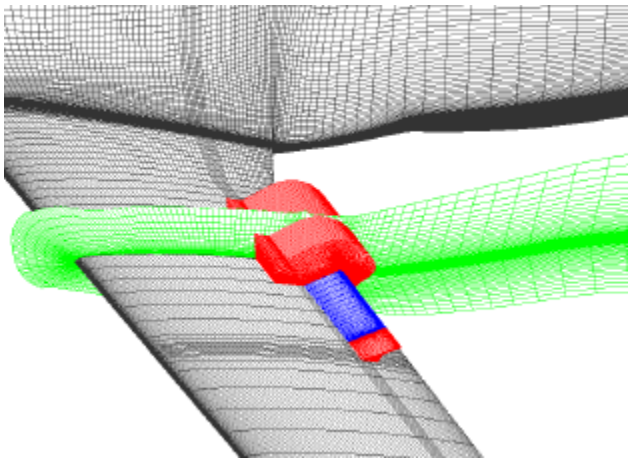

Fig. 20 Block-structured Chimera grid system for wing/body/spoiler configuration.

The component mesh was generated with the parametric grid generator MegaCads. Utilizing the scripting functionality of the software, a series of component meshes for different spoiler deflection angles were generated automatically. Due to the Chimera approach these component meshes could be easily positioned within the background mesh of the clean configuration. The main objective of this study was to investigate the complex flow phenomena around the spoiler. The flow around the spoiler is dominated by a blend of several vortices rotating around different axes. Fig. 21 shows

surface streamlines on the upper wing side. The dividing line that splits the flow in front of the spoiler into an inboard and outboard direction is visible close to the inboard spoiler end.

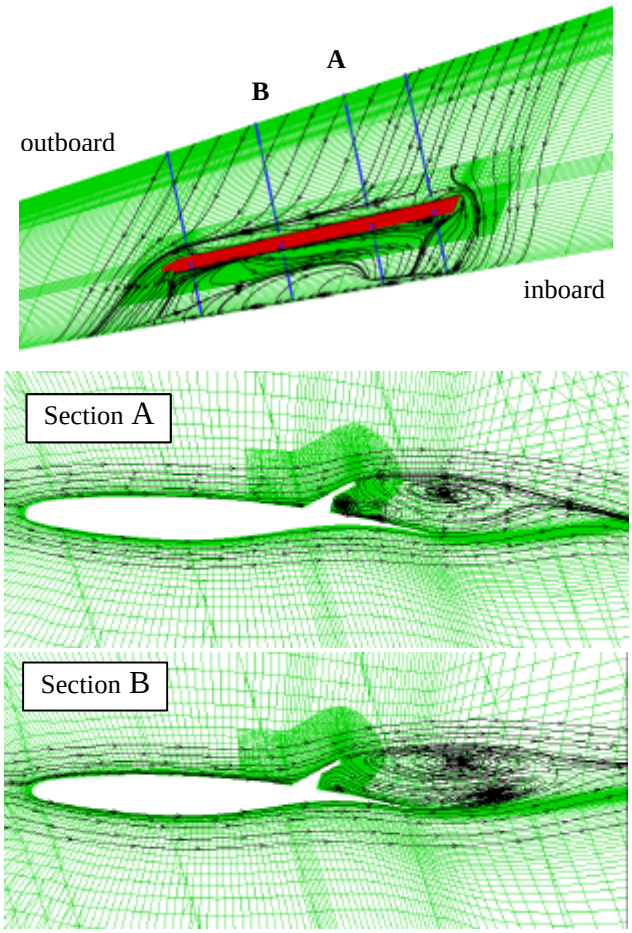

Fig. 21 Viscous calculation of wing/body/spoiler configuration using the Chimera option of FLOWer at M_∞=0.85, α=0^0, Re=8.1x10^6, streamlines on upper wing surface and two spoiler sections.

At the rear side of the spoiler a stagnation region due to flow separation is created forming different vortex patterns. This flow structure is also indicated by projected streamlines in two cross sections perpendicular to the spoiler. The investigations indicated that the MEGAFLOW simulation software is prepared to support the detailed understanding and assessment of active control surfaces.

The design and optimization of tail planes of large transport aircraft is also an important application area for numerical simulations. The TAU-Code with SAE was used [32] to predict the aerodynamic coefficients of a wing/body configuration with horizontal and vertical tail at M_∞=0.85 and Re=2.7x10^6. The hybrid grid consists of 8.7 million nodes. Fig. 22 shows the computed surface pressure in the rear part of the configuration. The comparison of measured and predicted pressure at a cross section of the horizontal tail close to the body is very good.

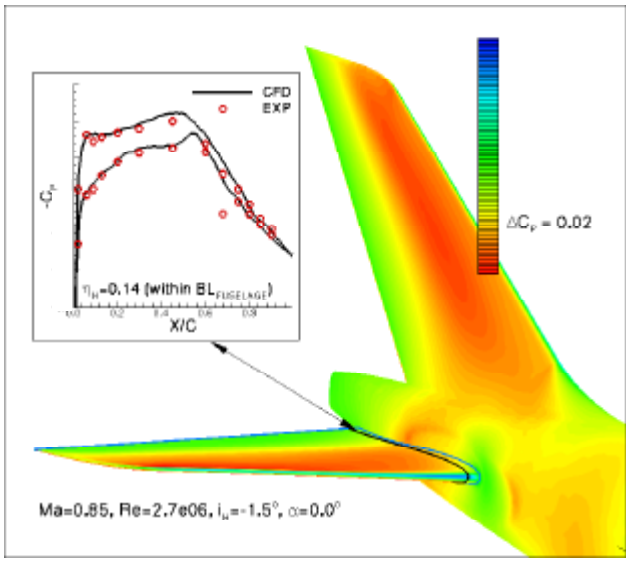

Fig. 22 Tail plane calculations with the hybrid Navier-Stokes solver TAU, surface pressure distribution in the rear part of the aircraft configuration.

In Fig. 23 drag and lift coefficients for the rear end (RE) of the configuration as a function of angle of attack are presented for different setting angles of the horizontal tail. The comparison with experimental data shows that the aerodynamic forces of tail planes can be predicted with high accuracy.

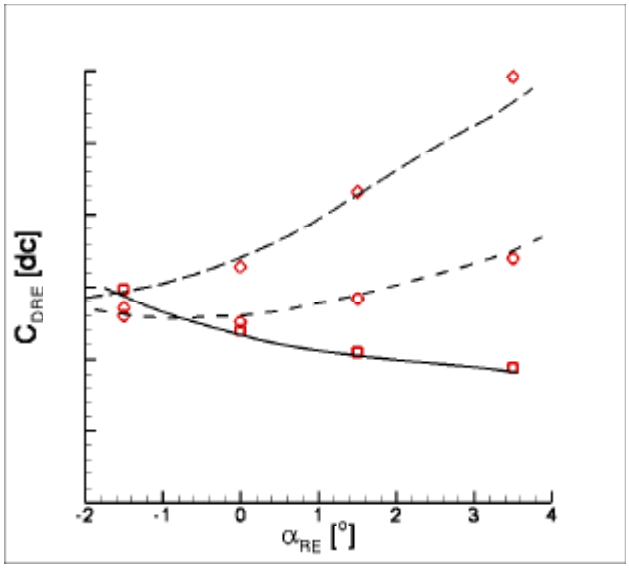

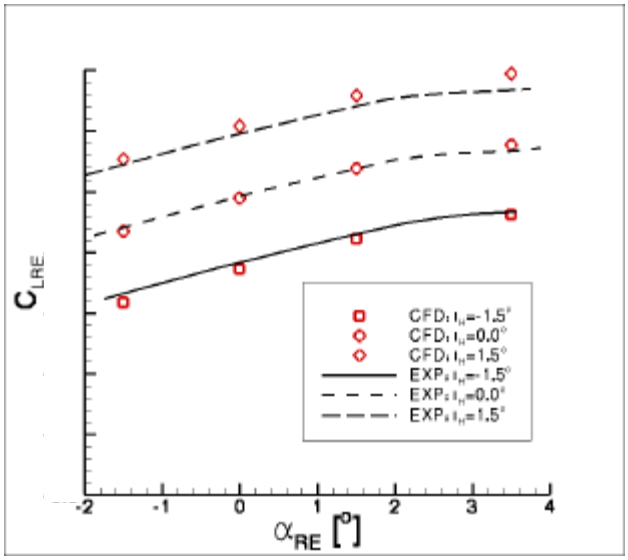

Fig. 23 Tail plane calculations with the hybrid Navier-Stokes solver TAU at M_∞=0.85, Re=2.7x10^6, lift (a)and drag coefficient (b) as function of angle of attack for different setting angles of horizontal plane.

For the regional jet aircraft Dornier DO 728, the potential of wing tip extensions to increase cruise performance was investigated [33]. The numerical tool employed was the FLOWer-Code, and computational meshes with C-H topology were used. Fig. 24 gives a view of the wing/body configuration with wing tip extension. For different wing tip extensions the corresponding surface pressure distributions are displayed. Note that for all configurations of the shark-family, no supersonic regions on the wing extension occurred. Fig. 24 also shows the improvement in drag reduction in percent compared to the standard wing without extensions. The performance predictions of the numerical study for the different configurations could clearly be confirmed by wind tunnel measurements.

5 Shape Design and Optimization

Aerodynamic shape optimization based on numerical methods is a key issue for future aircraft design. It offers the possibility of designing or improving aircraft components with respect to a prespecified figure of merit subject to geometrical and physical constraints.

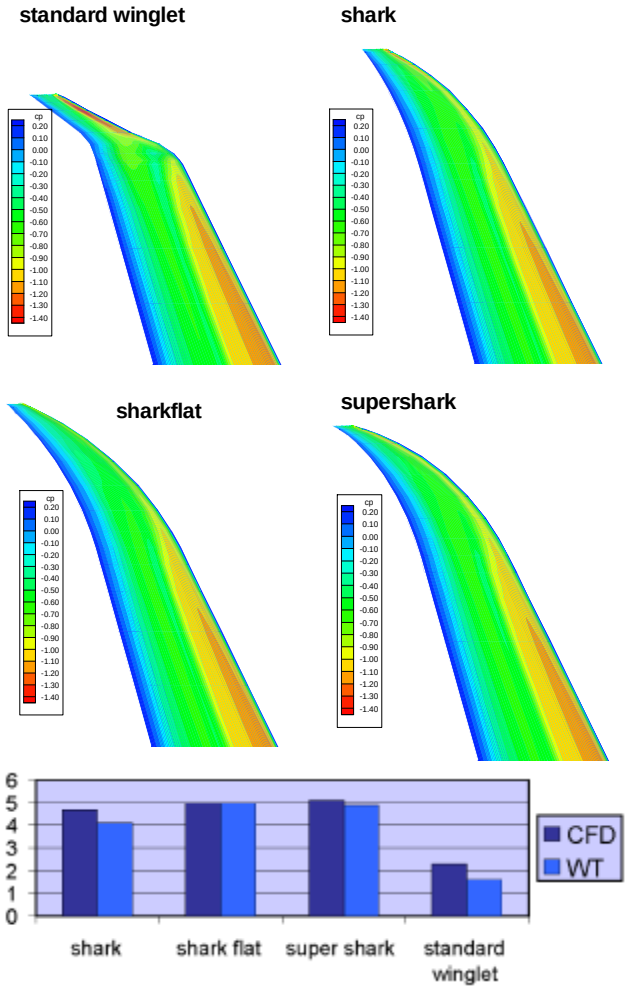

Fig. 24 Design study of wing tip extensions for DO 728 using the Navier-Stokes solver FLOWer, surface pressure distributions for different shapes, improvement in drag reduction in percent.

In the context of the DO 728/928 aircraft development various wing designs for transonic flow were performed at DLR with the inverse mode of the Navier-Stokes solver FLOWer. As design target suitable surface pressure distributions were specified subject to geometrical constraints and a given lift coefficient. Fig. 25 shows the comparison of drag rise between an early baseline wing and an improved wing as a function of Mach number. The reduction of drag in the higher Mach number range is clearly visible. The constraint with respect to the lift coefficient was satisfied.

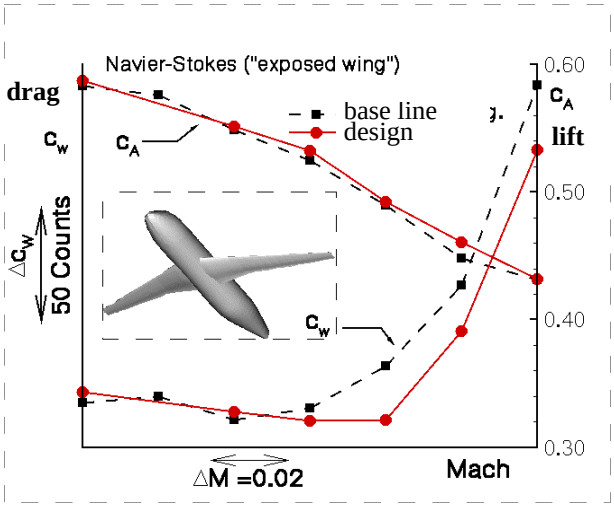

Fig. 25 Inverse wing design of a regional aircraft using FLOWer, drag rise and lift as function of Mach number for an early baseline configuration and optimized configuration.

The inverse design methodology based on the inverse formulation of the transonic small perturbation equations was also applied to the design of isolated and wing-mounted engine nacelles [35]. For these applications the inverse design module was coupled with the hybrid flow solver TAU. Fig. 26 shows results of the redesign of an installed nacelle. The aircraft geometry under consideration is the DLR ALVAST wing/body/pylon/nacelle configuration equipped with a VHBR engine. The initial nacelle geometry is set up by the scaled profiles of the side section only. The prescribed nacelle target pressure distribution corresponds to the surface pressure distribution of the installed VHBR nacelle. The redesign was performed for inviscid flow at M_∞=0.75, α=1.15^0 and the stream tube area ratio ε_{FAN}=0.96. Fig. 26 shows surface pressure distributions and nacelle profiles in three circumferential sections. As can be seen, the prescribed pressure distributions are met in all three sections. This demonstrates that the inverse design methodology is capable of designing installed engine nacelles.

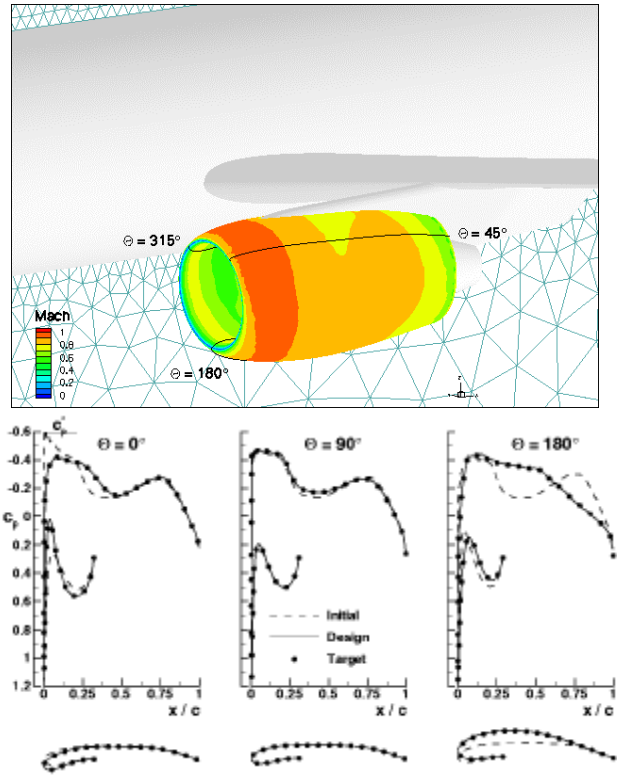

Fig. 26 Redesign of an installed nacelle using the TAU-Code, surface pressure distribution and nacelle profiles in three circumferential sections.

The design and improvement of high-lift systems open a wide area for the application of numerical optimization methods based on viscous RANS simulations. At DLR, large effort is devoted to this field. One important activity was to demonstrate that the optimization framework set up at DLR is able to detect optimal configurations determined by wind tunnel tests. The test case used for the validation of the optimization methodology is the NHLP L1T2 3-element airfoil. Contour lines of maximum lift coefficient $C_{L,max}$ as function of the slat position for a given deflection angle were experimentally determined at M_∞=0.197 and Re=3.52x10^6. The numerical optimization was performed with the block-structured FLOWer-Code using the Spalart/Allmaras turbulence model. For grid generation the DLR MegaCads system was employed. Using the batch mode, grid generation for the changed geometries is done automatically. Due the parametric concept of MegaCads grid quality is conserved for the different configurations that are evaluated during the optimization process.

The optimization strategy chosen for this test case is the downhill-simplex algorithm SUBPLEX [36].

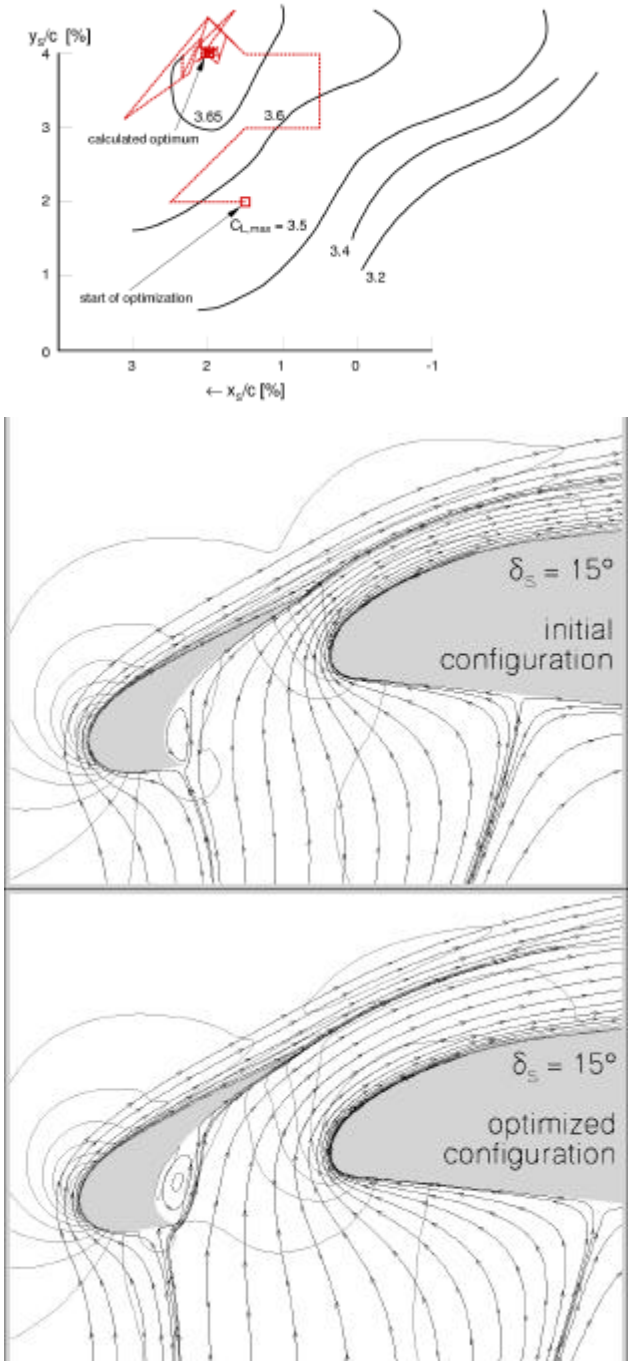

Fig. 27 Numerical optimization of 3-element-airfoil using the RANS solver FLOWer, (a) comparison of calculated optimum with experimentally determined contour lines of C_{LMAX}, (b) streamlines for initial and optimized geometry.

Fig. 27a shows the experimentally determined contour lines for a slat deflection angle of $\delta=15^0$ together with the search paths of the numerical optimization. It is obvious that the optimization strategy is able to detect properly the optimum location. Fig. 27b shows a comparison of the initial and optimal configuration. In the optimized configuration the slat has been pushed upwards resulting in a more uniform flow in the region of the slat wake. Furthermore, for the optimized configuration the stagnation point on the main airfoil is shifted downstream. The optimization strategy is used in many practical application, however, there is still large potential for further enhancements.

6 Spin - Off

Due to the low-speed capability of the TAU-Code it seems natural to utilize it also outside the aeronautical field and to apply it e.g. to the aerodynamics of ground-transport vehicles like cars, trucks and trains. Fig. 28 shows an example of the grid around a passenger car for which experimental data were made available after blind computations. Since the experiment employed a fixed floor with some boundary-layer suction (with an unknown suction rate) in an area upstream of the car the numerical simulation used a viscous wall only close to the car (gray area in Fig. 28) while the floor was otherwise treated as inviscid. The volume grid for the half configuration (assuming symmetry) composed of about 13.4 million prisms, tetrahedrons and pyramids contains 4.3 million grid points with 230.000 points on the surface.

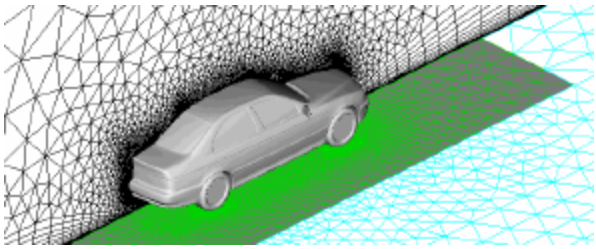

Fig. 28 Hybrid grid about BMW-type car on wind-tunnel floor, in symmetry plane and on car surface.

Fig. 29a provides some insight in the surface flow features like lines of separation and reattachment by means of simulated oil flow visualization in correspondence to the pressure distribution (with the high pressure areas

indicated by white/violet and low pressure areas by blue/green lines). During the numerical simulation the size of the prismatic elements was adapted to $Y^+=1$, but no refinement of the grid was performed. Fig. 29b shows that the computed and measured centerline pressure distribution match quite nicely, although discrepancies in the pressure above the rear window and trunk indicate that the separated vortical flow in that area is not yet sufficiently resolved. The drag coefficient was predicted within one percent of the experimental one.

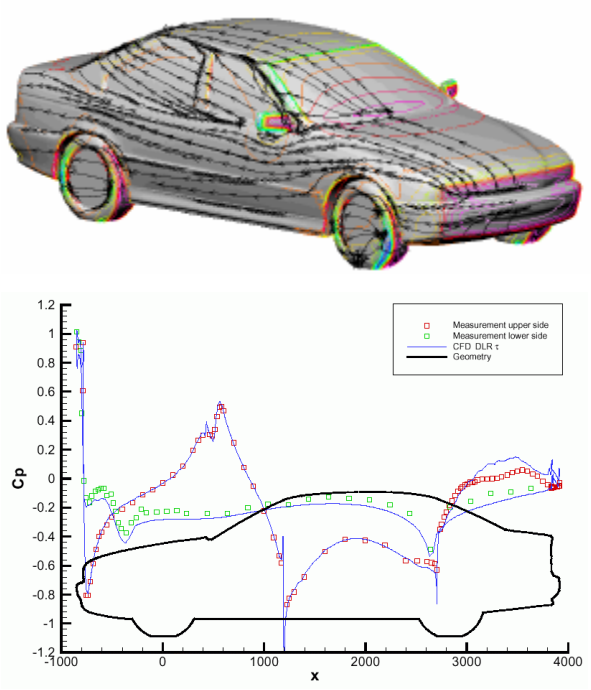

Fig. 29 Viscous calculations obtained with TAU-C, (a) surface streamlines and lines of constant surface pressure, (b) comparison of centerline pressure distribution between TAU results (lines) and experiment (symbols), figure courtesy of BMW.

7 Conclusions

The main objective of the MEGAFLOW initiative is the development of a dependable, effective and quality controlled program system for the aerodynamic simulation of complete aircraft. Due to its high level of maturity, the MEGAFLOW software system is being used extensively throughout Germany for solving complex aerodynamic problems – especially in industrial development processes. However, since industry is still demanding more accurate and faster simulation tools, further development is aimed at improvement of physical modeling, further reduction of problem turn-around time for large scale computations by advanced algorithms, enhancement of numerical optimization strategies as well as efficient integration of the MEGAFLOW tools into an efficient and flexible interdisciplinary simulation environment. Development activities in these directions have been initiated both on national and European level.

8 Acknowledgements

The authors would like to thank the following colleagues for providing the material presented in this paper: P. Aumann, O. Brodersen, B. Eisfeld, E. Elsholz, J. Fassbender, T. Gerhold, H. von Geyr, R. Heinrich, A. Krumbein, F. LeChuiton, A. Madrane, S. Melber, R. Mertins, M. Orlt, J. Raddatz, M. Rakowitz, R. Rudnik, A. Schütte, T. Schwarz, M. Sutcliffe, T. Streit, G. Vidjaja, C. Weber, G. Wichmann, J. Wild, R. Wilhelm.

9 References

[1] Kroll, N., Rossow, C.C., Becker, K., Thiele, F., MEGAFLOW - A Numerical Flow Simulation System, 21st ICAS Congress, paper 98-2-7.3, Mebourn, 1998.

[2] Kroll, N., Rossow, C. C., Becker, K., Thiele, F., The MEGAFLOW Project, Aerosp. Sci. Technol. Vol. 4, pp 223-237, 2000.

[3] Brodersen, O., Ronzheimer, A., Ziegler, R., Kunert, T., Wild, J., Hepperle, M., Aerodynamic Applications Using MegaCads, 6th International Conference on Numerical Grid Generation on Computational Field Simulations, Ed. M. Cross et al., ISGG, pp 793-802, 1998.

[4] Becker, K., Interactive Algebraic Mesh Generation for Twin Jet Transport Aircraft, Proc. 3rd Int. Conference on Num. Grid Generation, Barcelona, 1991.

[5] CentaurSoft, http://www.centaursoft.com/

[6] Heinrich, R., Ahrem, R., Günther, G., Kersken, H.-P., Krüger, W., Neumann, J., Aeroelastic Computation Using the AMANDA Simulation Environment, Proc. of CEAS Conference on Multidisciplinary Aircraft Design and Optimization, pp. 19-30, Köln, Germany, 2001.

[7] http://www.mpcci.org/

[8] Kroll, N., Radespiel, R., Rossow, C.-C., Accurate and Efficient Flow Solvers for 3D-Applications on Structured Meshes, AGARD R-807, 4.1-4.59, 1995.

[9] Aumann, P., Barnewitz, H., Schwarten, H., Becker, K., Heinrich, R., Roll, B., Galle, M., Kroll, N., Gerhold, Th., Schwamborn, D., Franke, M., MEGAFLOW: Parallel Complete Aircraft CFD. Parallel Computing, Vol. 27, pp 415-440, 2001.

[10] Rung, T., Lübcke, H., Franke, M., Xue, L., Thiele, F., Fu, S., Assessment of Explicit Algebraic Stress Models in Transonic Flows, Proceedings of the 4th Symposium on Engineering Turbulence Modeling and Measurements, France, pp. 659-668, 1999.

[11] Kok, J.C., Brandsma, F.J., Turbulence Model Based Vortical Flow Computations for a Sharp Edged Delta Wing in Transonic Flow Using the Full Navier-Stokes Equations, NLR-CR-2000-342, 2000.

[12] Wallin, S., Johansson, A.V., An Explicit Algebraic Reynolds Stress Model for Incompressible and Compressible Turbulent Flows, J. Fluid Mech., Vol. 403, pp. 89-132, 2000.

[13] Rakowitz, M., Sutcliffe, M., Eisfeld, B., Schwamborn, D., Bleecke, H., Faßbender, J., Structured and Unstructured Computations on the DLR-F4 Wing-Body Configuration, AIAA 2002-0837, 2002.

[14] LeChuiton, F., Actuator Disc Modeling for Rotory Wings, 28th European Rotorcraft Forum, Bristol, England, 2002.

[15] Krumbein, A., Coupling of the DLR Navier-Stokes Solver FLOWer with an e^N-Database Method for Laminar-Turbulent Transition Prediction on Airfoils, Notes on Numerical Fluid Mechanics, Vol. 77, pp. 92-99, 2002.

[16] Heinrich, R., Kalitzin, N., Numerical Simulation of Three-Dimensional Flows Using the Chimera Technique, Notes on Numerical Fluid Mechanics, Vol. 72, Vieweg Braunschweig, pp. 15-23, 1999.

[17] Schwarz, Th., Development of a Wall Treatment for Navier-Stokes Computations Using the Overset Grid Technique, 26th European Rotorcraft Forum, Paper 45, 2000.

[18] Takanashi, S., Iterative Three-Dimensional Transonic Wing Design Using Integral Equations, Journal of Aircraft, Vol 22, No 8., 1985.

[19] Bartelheimer, W., An Improved Integral Equation Method for the Design of Transonic Airfoils and Wings, AIAA 95-1688,1995.

[20] Jameson, A., Martinelli, L., and Pierce, N., Optimum Aerodynamic Design Using the Navier-Stokes Equations. Theoret. Comput. Fluid Dynamics, Vol 10, pp. 213-237, 1998.

[21] Gauger, N., Brezillon, J., Aerodynamic Shape Optimization Using Adjoint Method, Journal of the Aeronautical Society of India, to appear in 2002.

[22] Gerhold T., Friedrich, O., Evans J., Galle, M., Calculation of Complex Three-Dimensional Configurations Employing the DLR-TAU Code, AIAA 97-0167, 1997.

[23] Schütte, A., Einarsson, G., Madrane, A., Schöning, B., Mönnich, W., Krüger, W.-R., Numerical Simulation of Maneuvering Aircraft by CFD and Flight Mechanic Coupling, RTO Symposium, Paris, April, 2002.

[24] http://www.aiaa.org/tc/apa/dragpredworkshop/dpw.html.

[25] Monsen, E., Franke, M., Rung, T., Aumann, P., Ronzheimer, A., Assessment of Advanced Transport-Equation Turbulence Models for Aircraft Aerodynamic Performance Prediction, AIAA 99-3701, 1999.

[26] Rudnik, R., Melber, S., Ronzheimer, A., Brodersen, O., Three-Dimensional Navier-Stokes Simulations for Transport Aircraft High Lift Configurations, Journal of Aircraft, Vol. 38, pp. 895-903, 2001.

[27] Rudnik, R., Towards CFD Validation for 3D High Lift Flows – EUROLIFT, ECCOMAS 2001, Swansea, United Kingdom, 2001.

[28] Melber, S., Wild, J.; Rudnik, R., Overview about the NLRS-Project on Numerical High Lift Research, DLR-IB 124, 2002/15, 2002.

[29] Brodersen, O., Stürmer, A., Drag Prediction of Engine-Airframe Interference Effects Using Unstructured Nvier-Stokes Calculations, AIAA 2001-2414, 2001.

[30] Rudnik, R., Rossow, C.C., v. Geyr, H., Numerical Simulation of Engine/Airframe Integration for High-Bypass Engines, Aerosp. Sci. and Technol., Vol. 6, pp 31-42, 2002.

[31] Mertins, R., Barakat, S., Elsholz, E., 3D Viscous Flow Simulation on Spoiler and Flap Configurations, CEAS Aerospace Aerodynamics Research Conference, Paper No. 65, Cambridge, United Kingdom, 2002.

[32] Weber, C., 3D Navier-Stokes-Berechnungen an einer A380-Leitwerkskonfiguration, Airbus Report, EGAG-237/02, 2002.

[33] Heller, G., Dirmeier, S., Kreuzer, P., Streit, Th., Aerodynamische Leistungssteigerung durch Flügel-spitzenmodifikationen am Beispiel der Envoy 7, DGLR Symposium Paper No. 2001-103, 2001.

[34] Streit, Th., Wichmann, G., Rohard, C.H., Nachrechnung und Entwurf von transsonischen Tragflügeln für die DO-728 / DO-928, DLR IB 129-99/13, 1999.

[35] Wilhelm, R., An Inverse Design Method for Designing Isolated and Wing-Mounted Engine Nacelles, AIAA 2002-0104.

[36] Wild, J., Validation of Numerical Optimization of High-Lift Multi-Element Airfoils based on Navier-Stokes-Equations, AIAA 2002-2939, 2002.